CR-171740
C.1

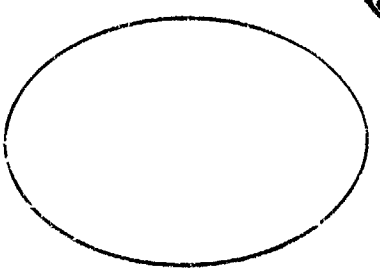

TEXAS ENGINEERING EXPERIMENT STATION

The Texas A&M University System

COLLEGE STATION, TEXAS 77843

SPACE SHUTTLE ICE SUPPRESSION
SYSTEM VALIDATION
TEES-TR-4587-82-01
VOLUME I

J.L.F. PORTEIRO, D.J. NORTON
AEROSPACE ENGINEERING DEPARTMENT
AND
T.C. POLLOCK
ENGINEERING DESIGN AND GRAPHICS DEPARTMENT

Prepared for
NASA Lyndon B. Johnson Space Center
Thermal Technology Branch
Houston, Texas 77058
Under Contract NAS 9-16443

Prepared by
Texas Engineering Experiment Station
Texas A&M University
College Station, Texas 77843

TABLE OF CONTENTS

LIST OF FIGURES

LIST OF TABLES

INTRODUCTION

The loading of cryogenic propellants into the Space Shuttle External Tank (ET) may result in the formation of ice on its surface. Such ice formation poses a potential threat to the Thermal Protection System (TPS) tiles of the Shuttle Orbiter as a substantial number of chunks of ice may be dislodged on liftoff, impact the tiles and damage them. It is therefore desirable to prevent the formation of ice on the surface of the external tank.

It has been proposed that such formation can be prevented by using turbojet engines exhausts. The jet exhausts would be arranged in such a way that they would generate a temperature and velocity field such that the heat transfer coefficient on the surface of the ET would be sufficient to prevent ice formation.

The main objective of the research program carried out at Texas A&M was to establish the effectiveness of the jet exhaust arrangement proposed by Norman Engineering Company in generating such a flow field. A secondary objective was the study of similar arrangement proposed by the Marshall Space Flight Center for the same purpose.

RESEARCH PROGRAM

The research involved in the evaluation of the Ice Suppression System (ISS) was carried out in two phases. Phase I involved the preliminary analytical considerations needed to establish a successful experimental program, as well as the experimental investigation of the flow field for the desired configurations in the absence of wind effects. Phase II was a wind tunnel test program using the information

acquired in Phase I to determine the effect of different wind conditions on ISS performance.

ISS CONFIGURATIONS

Three different configurations (or arrangements) were studied in this program. They will be referred to in the test as the Nominal, Variable size nozzle array and Marshall configurations.

Nominal Configuration

The nominal nozzle configuration used the geometrical arrangement proposed by Norman Engineering in its Concept Summary Report, Volume I, Figure A-4. It is characteristic of this configuration that all twelve nozzles used at the same time are the same size. Three sets of converging nozzles were considered to study nozzle size effects. They were:

Large: 1.698 ft. diameter

Nominal: 1.104 ft. diameter

Small: 0.770 ft. diameter

It is necessary, then, to specify nozzle size when referring to the Nominal configuration.

Variable Size Nozzle Array Configuration

This configuration differs from the Nominal only in that different nozzle sizes are used simultaneously. Nozzle size arrangement was as follows:

Small Nozzle Size: Lower three locations on each tower (1, 2, 3 and 1A, 2A and 3 as shown in Figure 1).

Nominal Nozzle Size: Nozzles No. 4 and 5 on each tower.

Large Nozzle Size: Nozzle No. 6 on each tower.

NOZZLE LOCATIONS

AND

INCIDENCE ANGLES

FOR

NORMAN ENGINEERING

CONFIGURATIONS

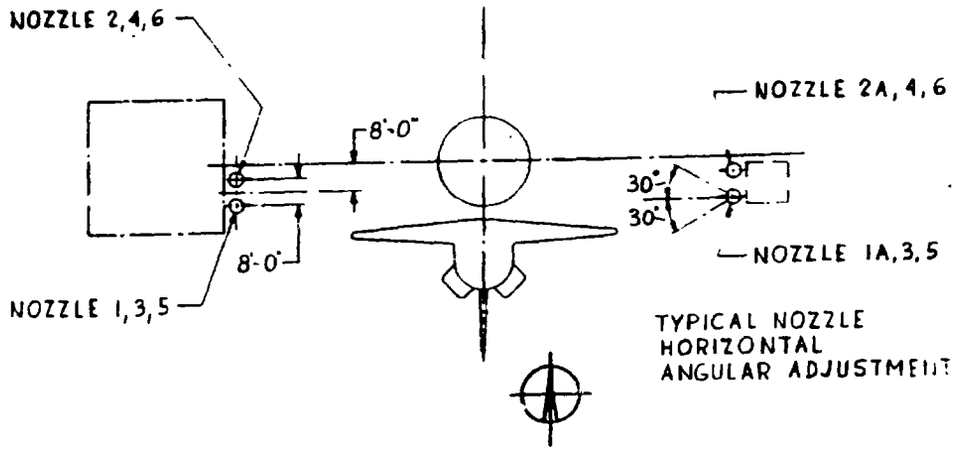

SSAT	
NOZZLE No.	INCIDENCE ANGLE
1	1°
2	16°
3	20°
4	34°
5	35°
6	49°

IST	
NOZZLE No.	INCIDENCE ANGLE
1A	13°
2A	27°
3	20°
4	34°
5	35°
6	49°

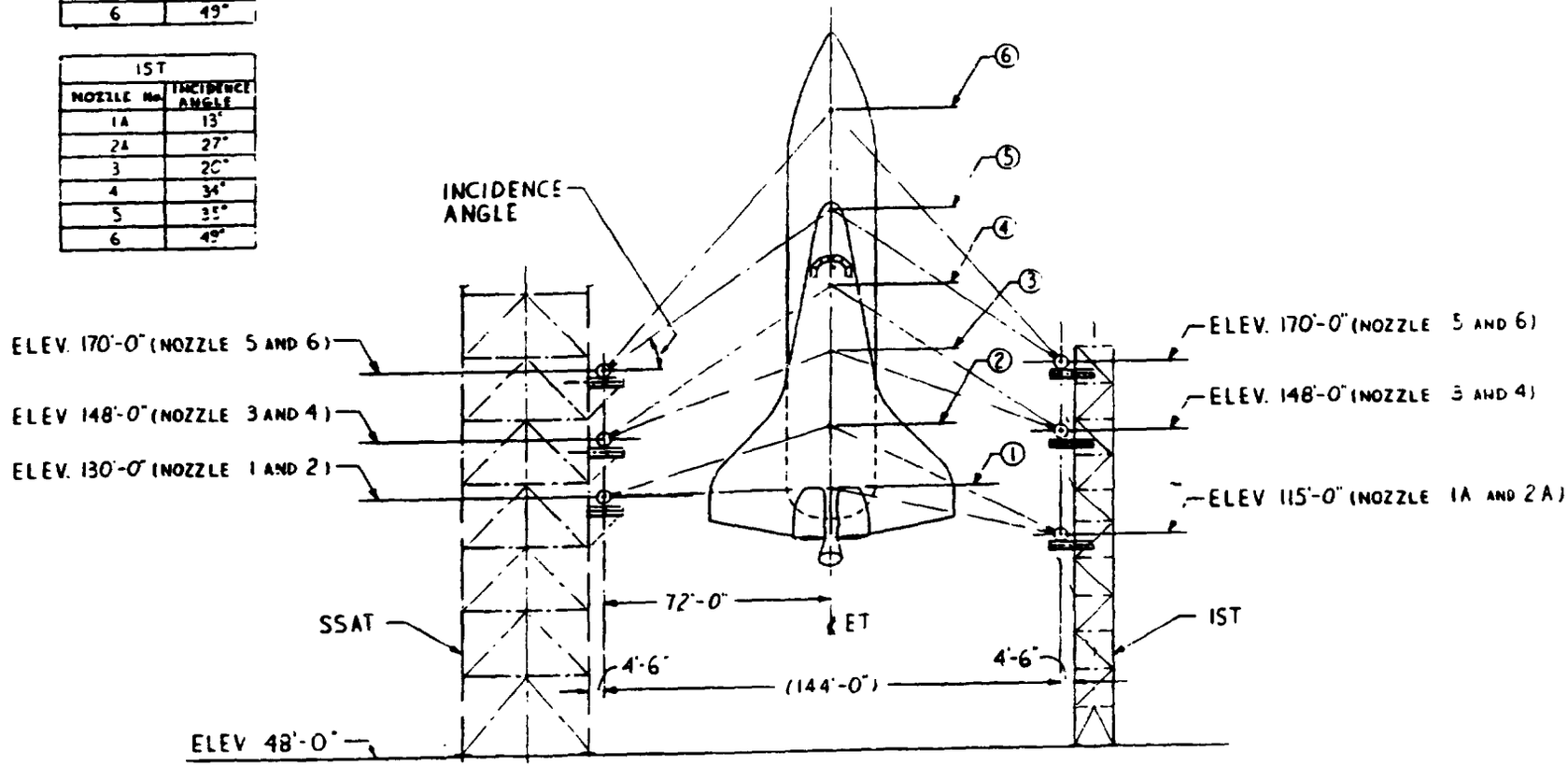

FIGURE 1

Marshall Space Flight Center Configuration

The Marshall configuration involves the use of four vertical jets mounted on the surface of mobile launch platform (MLP) on a circle, at 90° intervals as shown in Figure 2. Tests were conducted for two nozzle sizes and conditions: 3.0 ft. diameter and 217 lbm/sec. per jet and 1.7 ft. diameter and 82 lbm/sec. per jet.

TEST CONDITIONS

Model Details

Using detailed drawings provided by NASA and Rockwell International, a detailed 2% replica of all relevant structural features of KSC Launch Complex 39A was designed and built. At the same time the necessary hardware was fabricated to incorporate scaled down ISS's as proposed by Norman Engineering and MSFC.

Two different shuttle models were used for testing. A high fidelity 2% STS wind tunnel model was instrumented with 119 pressure ports and used for pressure and velocity measurements. For the purposes of flow visualization a second model was built incorporating all ET details relevant to a successful simulation. Both the planform and underside contour of the orbiter were reproduced.

Wind Velocity Profile

A "1/7" power law wind velocity profile representing the Earth's boundary layer was used. Wind tunnel flow was "tailored" by using a "fence" with various rods to produce a scaled velocity profile matching the velocity-height relationship for the launch site. The wind velocity profile was substantiated through the use of a vertically traversing pitot-static probe, and is presented in Fig. 3.

MARSHALL SPACE FLIGHT CENTER

CONFIGURATION

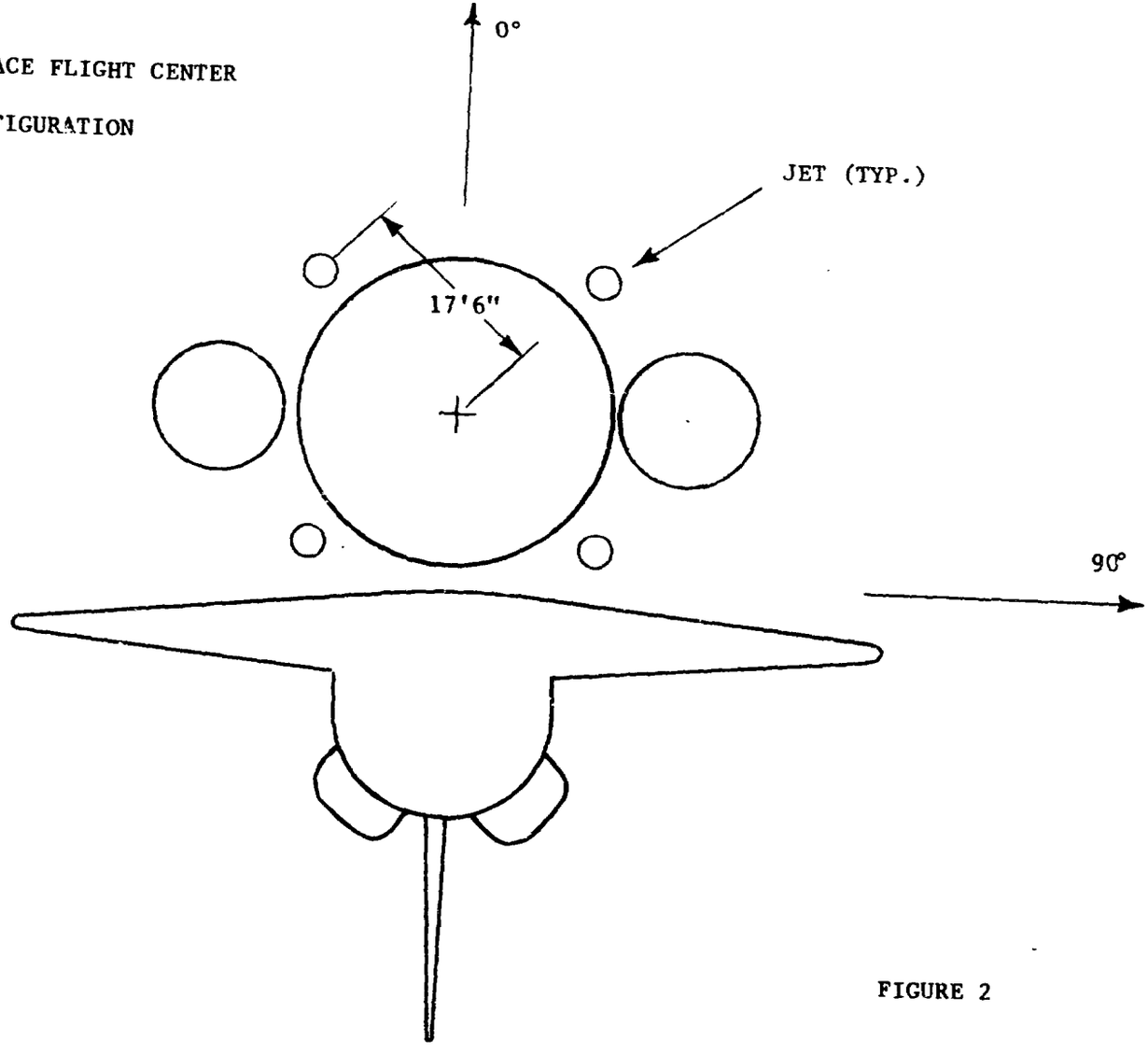

FIGURE 2

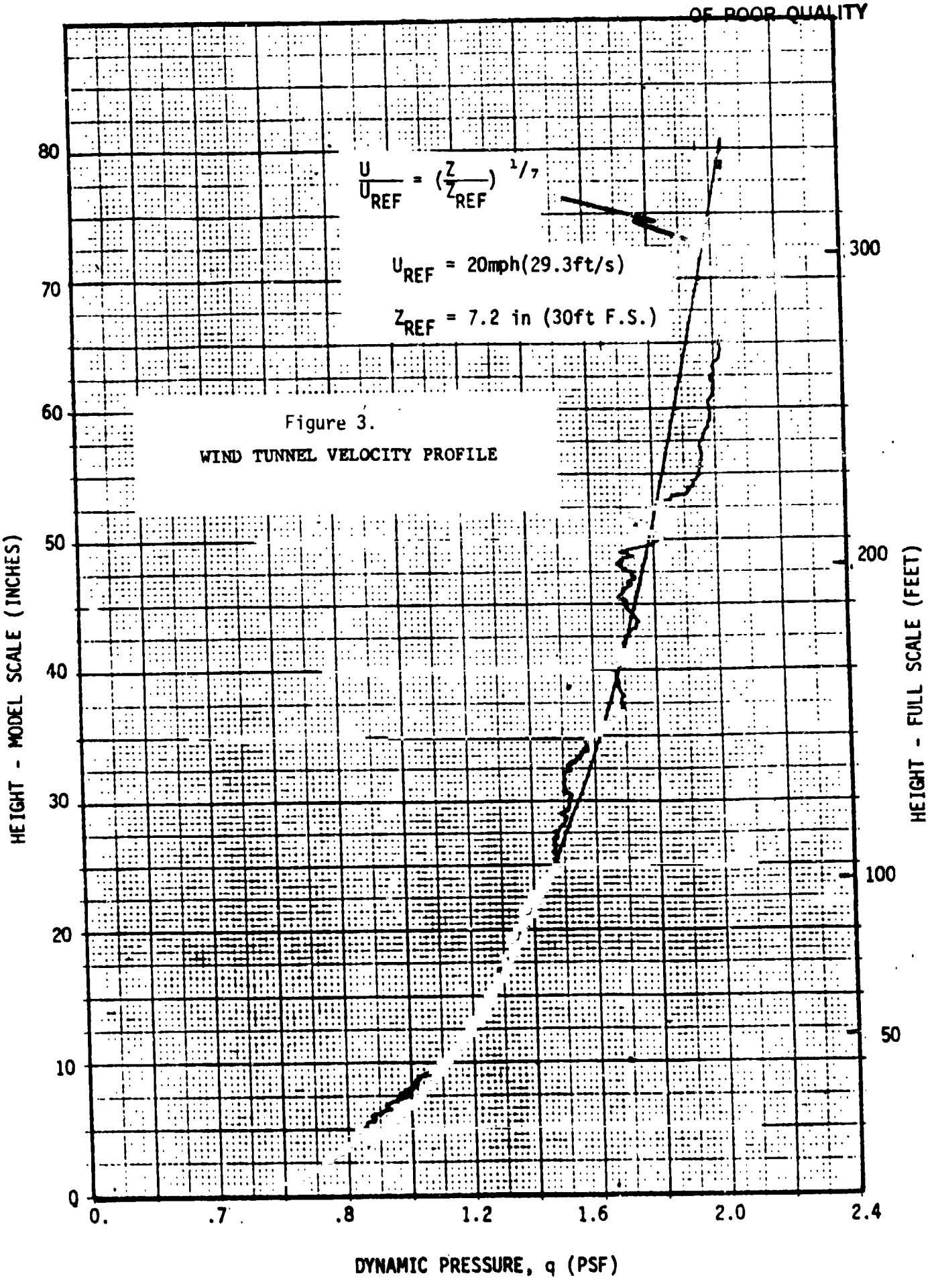

Figure 3.

WIND TUNNEL VELOCITY PROFILE

A range of dynamic pressures representing ground winds ranging from 7 to 30 knots at a full scale height of 30 feet was used.

Wind Direction

Different wind directions were simulated by rotating the Pad complex and Shuttle model around the ET centerline. The predominant winter wind direction (333°) and summer directions (202° and 112°) were studied.

Other Variables

The Norman Engineering design has the capability of improving wind penetration by altering nozzle pressure and azimuth angle. The test model used also possessed this capability and therefore, tests were made at different pressures and nozzle azimuth angles. Tests were conducted for three nozzle stagnation pressures: 32, 27 and 20 psia. The nozzle azimuth angle was varied as much as 30° from the 0° position as shown in Figure 1.

SCALING LAWS

The objective of this wind tunnel program was the simulation of the velocity field around the Shuttle Launch configurations and evaluations of jet planes interaction with different wind direction; no heat transfer measurements were to be made.

The minimum distance between the nozzle exit and the ET centerline is always 60 diameters or more for the Norman Engineering design; thereby alleviating the requirement for a detailed simulation of the near field. The velocity field will be similar to that of the full scale configuration, if the momentum of the jets is properly scaled.

The momentum at the nozzle of the jet can be written as

$$\text{Mom.} = \tfrac{1}{2} \int_0^A \rho V^2 dA = \tfrac{1}{2} \int_0^A \frac{p}{RT} M^2 KRT \, dA = \frac{K}{2} \int_0^A pM^2 dA$$

If p_e and M_e are the values of p and M averaged over A then

$$\text{Mom.} = \frac{K}{2} p_e M_e^2 A$$

If the flow is choked $M_e = 1$ thereby reducing relations to

$$\text{Mom.} = \frac{K}{2} p_o \frac{p_e}{p_o} A = 0.528 \frac{K}{2} p_o A$$

where p_o is the stagnation pressure. If the flow is subsonic Mach number becomes dependent on pressure ratios yielding

$$M_e = f\left(\frac{p_e}{p_o}\right) = f\left(\frac{p_{at}}{p_o}\right) = f(p_o)$$

and $$\text{Mom.} = \frac{K}{2} p_o f(p_o) A$$

As it can be seen, to scale momentum all that needs to be done is to scale the physical dimensions of the nozzle linearly while keeping the stagnation pressure unchanged. On the other hand, the centerline velocity of a jet decays with distance according to the formula

$$\frac{U_{CL}}{U_o} = \frac{\text{Constant}}{x/d}$$

where: U_{CL} is the velocity at the centerline of the jet;

U_o is the velocity at the nozzle exit;

d is the diameter of the nozzle;

x is the distance from the nozzle exit along the jet centerline.

Since nozzle diameter scales linearly as it was seen above, the only other requirement to adequately simulate the jet flow field is to scale all other dimensions linearly as well.

The flow field to be simulated is highly turbulent. A linear scaling of the type mentioned above will also result in an adequate simulation of both the turbulent length scale and turbulence level of the flow field.

This is based on the fact that the turbulent length scale is a function of nozzle diameter while turbulence intensity is only a function of the ratio x/d.

It should be noted that the additional turbulence generated by the interaction of the jets is such that flow field properties are basically independent of Reynolds number.

This is indeed fortunate since adequate simulation of jet-wind interaction requires that the ratios of wind velocity to jet velocity remain fixed and thus condition makes a Reynolds number simulation between model and full scale impossible.

For the purposes of the tests carried out in this research program this is of no consequence since the measurements made and the phenomena studied are basically Reynolds number independent. The flow field under study, as indicated above, is inherently highly turbulent.

EXPERIMENTAL PROGRAM

Three different techniques were used for the investigation of the flow field around the Pad complex and the Shuttle model:

Flow Visualization techniques were used to provide a qualitative picture of the flow field around the ET and Orbiter underside. An adequate number of test conditions were studied to provide information on the influence of the different test parameters on flow field patterns.

Pressure Measurements were made on the ET surface to provide quantitative information on the influence of test parameters on the pressure field around the ET. Such information may be useful in studying trends and establishing the effects of different parameters.

Hot Film measurements of velocity, turbulence level and temperature were made. These measurements can provide direct confirmation of the high level of turbulence that is expected in this type of flow field. The velocity measurements, even though not accurate in many cases due to the high levels of turbulence, provide an indication of the magnitude of the velocity and may be used to study trends and the effects of different test parameters. Temperature measurements should provide useful information for heat transfer studies.

FLOW VISUALIZATION STUDIES

Flow visualization studies were carried out both in the lab and in the wind tunnel. Much of the preliminary lab activity involved the development of an effective testing procedure and the preparation of a flow visualization liquid suitable for the range of velocities predominant in the tests.

After numerous tries with different liquids and dyes it was decided that a mixture of black tempra paint and kerosene gave best results. An added advantage of this mixture was its easy manufacturing and handling. Its viscosity can be controlled by the addition of kerosene or paint. White lacquer paint was used to paint the flow visualization model. This type of paint was used for two reasons:

a) It is not affected by kerosene and

b) The mixture could be easily wiped off after a test, providing quick turn-around times.

The region of the ET facing the Orbiter was one of the key areas to be investigated. For this purpose, a method of removing and installing the Orbiter quickly was devised.

Suitable photographic procedures were also devised in order to provide good quality photographs. It is important to note that space limitations and lighting conditions made the task very difficult inside the wind tunnel test section; nevertheless, excellent quality photographs were obtained.

Procedure

The first step on a normal test run involved "painting" the Shuttle Launch Configuration with the flow visualization mixture, which had previously been checked for viscosity. Last part of this step was the "painting" of the Orbiter underside and the mounting of the Orbiter on the ET. Wind tunnel and jet flow were started immediately after this to prevent the mixture from drying up on the model. The tests were run for times long enough to establish a steady flow field pattern and blow off all excess liquid. The mixture had a tendency

to accumulate on the ET ogive so it was important to wait for most of the accumulated liquid to blow off as, upon shutting down jets and tunnel, this liquid would flow back down due to gravity and it would smear the flow field patterns on the ET.

As soon as the tunnel and jets were shut down, the Orbiter was removed from the ET and the photographer proceeded to photograph the flow patterns on both sides of the ET before any significant backflow took place. The last task of a run was the cleaning and preparation of the model for the next run.

Cases Studied

A total of 38 tests were made to study the influence of four parameters: wind direction, wind velocity, nozzle pressure and nozzle azimuth angle on the flow field patterns generated by the three ISS configurations. Tables 1, 2, 3 and 4 show all the parameters pertinent to the tests. As can be seen the range of the parameters tested was as follows:

Wind Direction:	112°, 202° and 338°
Wind Velocity:	0, 7, 10, 20 and 30 knots
Nozzle Pressure:	0, 20, 27 and 32 psia
Nozzle Azimuth Angle:	0°, -15° and -30°

It was not possible to run all possible combinations of the above mentioned parameters, so the most significant combinations were run in such a way that the influence of each parameter could be studied independently. The influence of different parameters can be investigated by studying the following groups of runs:

Nominal Arrangement

I) Nozzle size influence, no wind

Runs A, B and C or D, E and F or G, H and I

II) Nozzle pressure influence, no wind

Runs A, D and G or B, E and F or C, F and I.

III) Wind direction effect at 20 KT

Runs 13, 14 and 17

IV) Wind vecolity effects at 112°

Runs 1, 8 and 19

V) Wind velocity effects at 202°

Runs 2, 15 and 16

VI) Wind velocity effects at 338°

Runs 3, 4 and 5

VII) Nozzle pressure effects at 20 KT and 338°

Runs 3, 6 and 7

VIII) Nozzle azimuth angle effects at 20 KT and 338°

Runs 3, 8 and 9

IX) Wind velocity/Azimuth angle interaction

Runs 9 and 10

X) Influence of nozzle pressure on wind penetration

Runs 10, 11 and 12

Marshall Space Flight Center Configuration

I) Flowrate effects, no wind

Runs 44 and 47

II) Wind velocity effects at high flowrate

Runs 44, 45 and 46

Variable Nozzle Size Configuration

I) Nozzle pressure effects, no wind

Runs 48, 49 and 50

II) Influence of nozzle pressure on wind penetration

Runs 51, 52 and 53

ET SURFACE PRESSURE MEASUREMENTS

A total of 54 wind tunnel test runs were made for the purpose of determining ET surface pressure in a wide variety of test conditions. All three nozzle arrangements were studied. The main purpose of the pressure surveys was the determination of stagnant or separated flow regions, and the study of the different test parameters on the ET pressure field.

Procedure

As previously mentioned a total of 119 pressure taps were installed on the ET surface. Figures 4 and 6 show both the details of the simulated ET surface and the location of all pressure taps located in the surface of the ET facing the Orbiter. Each tap was connected to one of three scanivalves mounted inside the ET. Each scanivalve was capable of handling 48 different pressure ports. This capability allowed the use of five ports on each scanivalve to provide reference and calibration pressures. Pressure ports 0, 23 and 47 were used for the reference pressure and ports 1 and 24 were supplied with a calibration pressure. Each scanivalve was connected to a pressure transducer providing a voltage proportional to the difference between the pressure to be measured and the reference pressure. The test section of the wind tunnel is kept at atmospheric

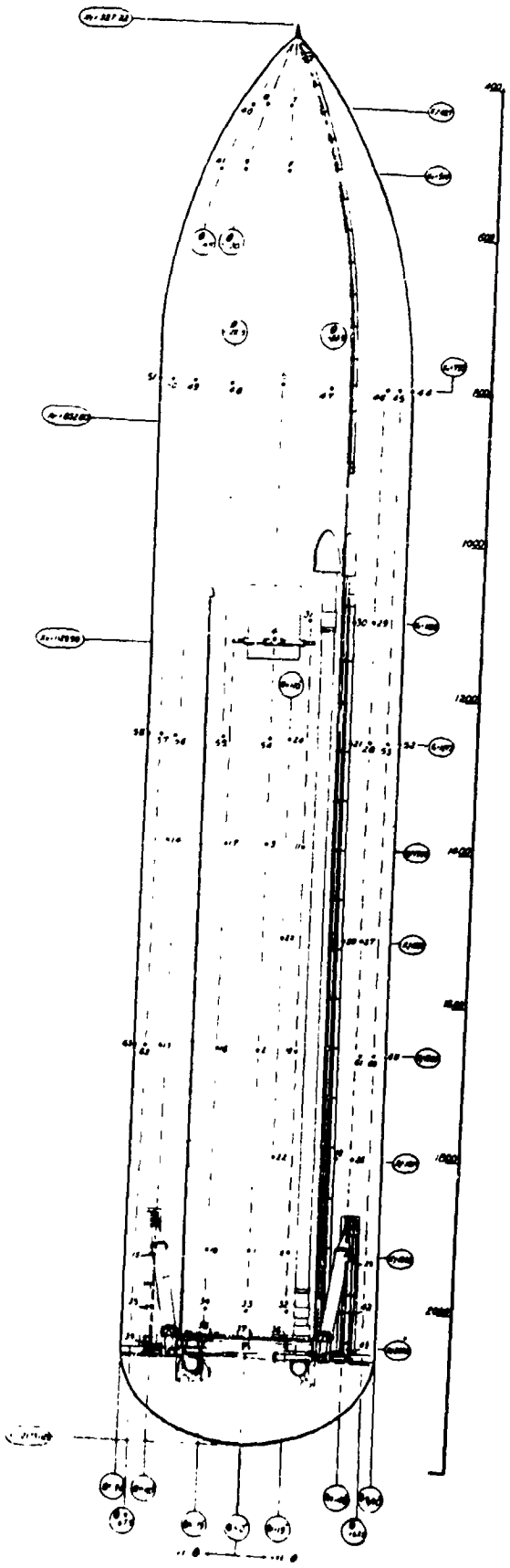

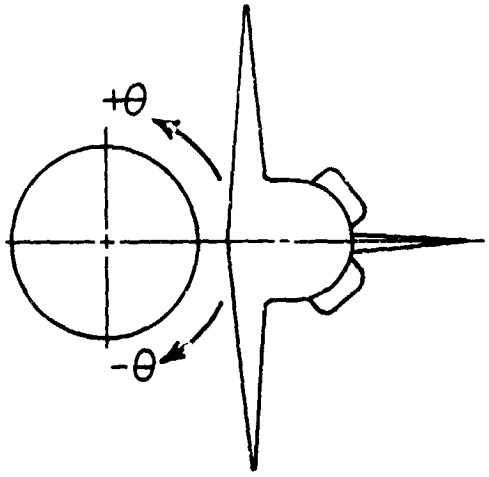

Figure 4. E.T. Pressure Tap Locations

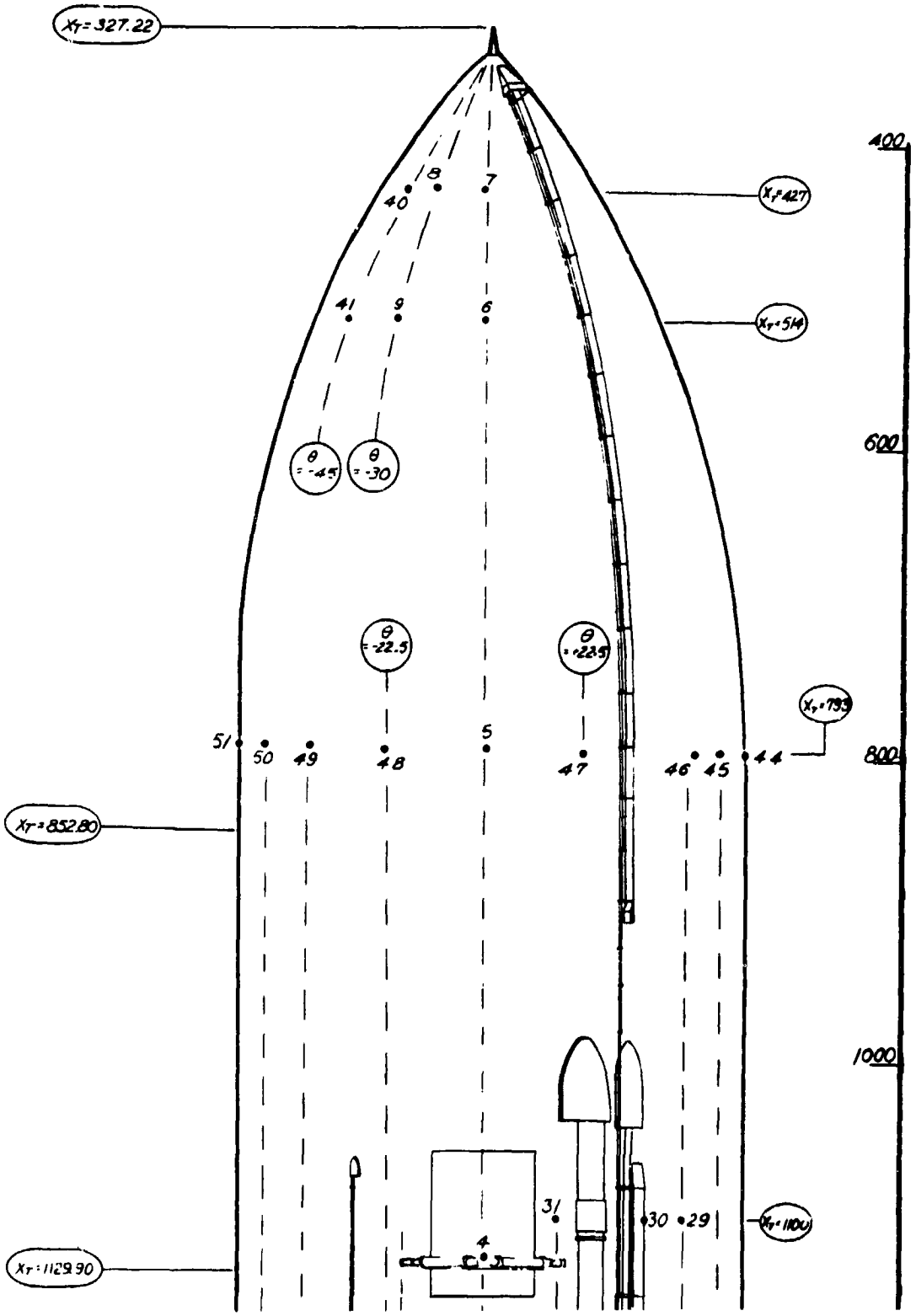

Figure 4. Continued

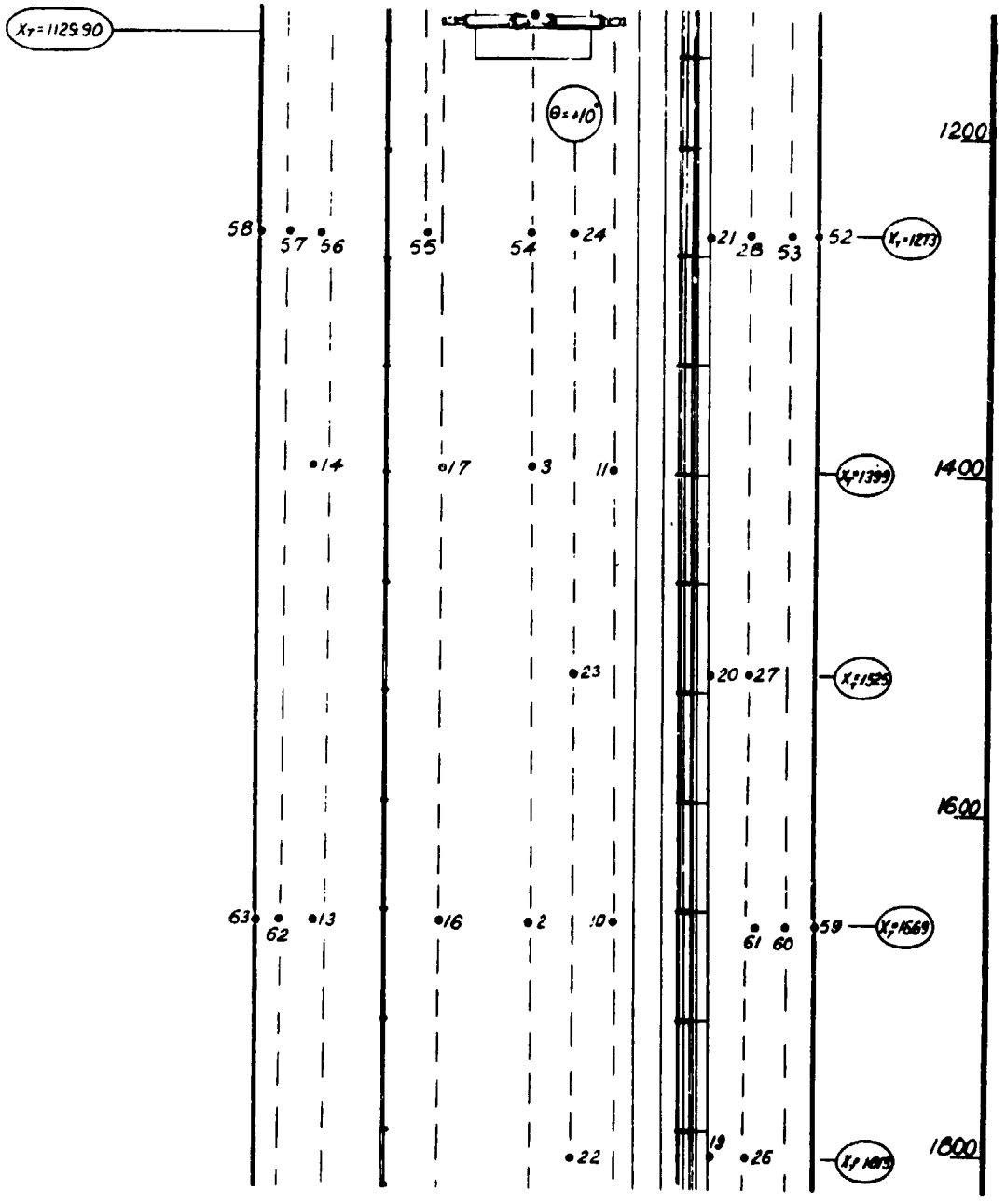

Figure 4. Continued

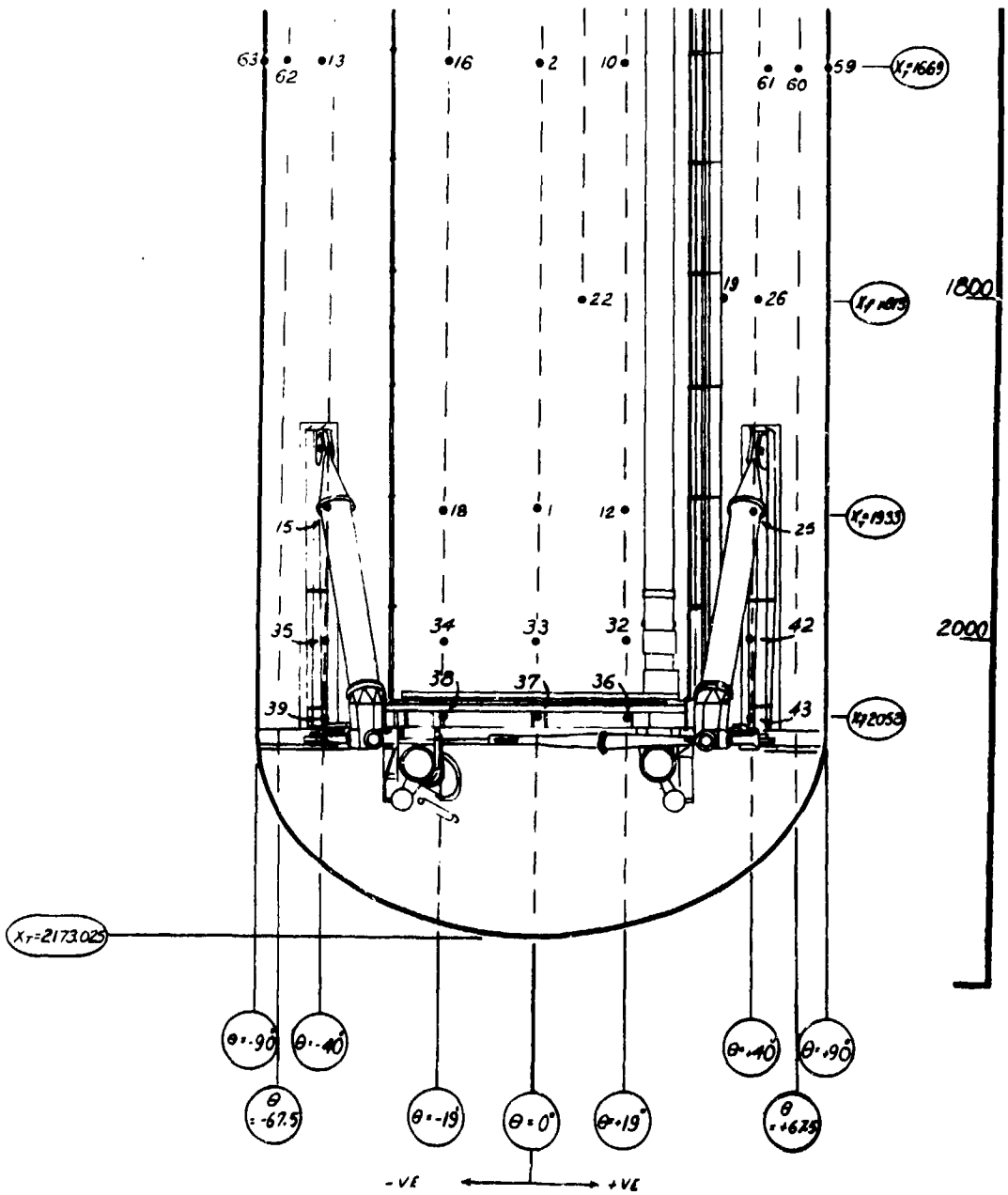

Figure 4. Continued

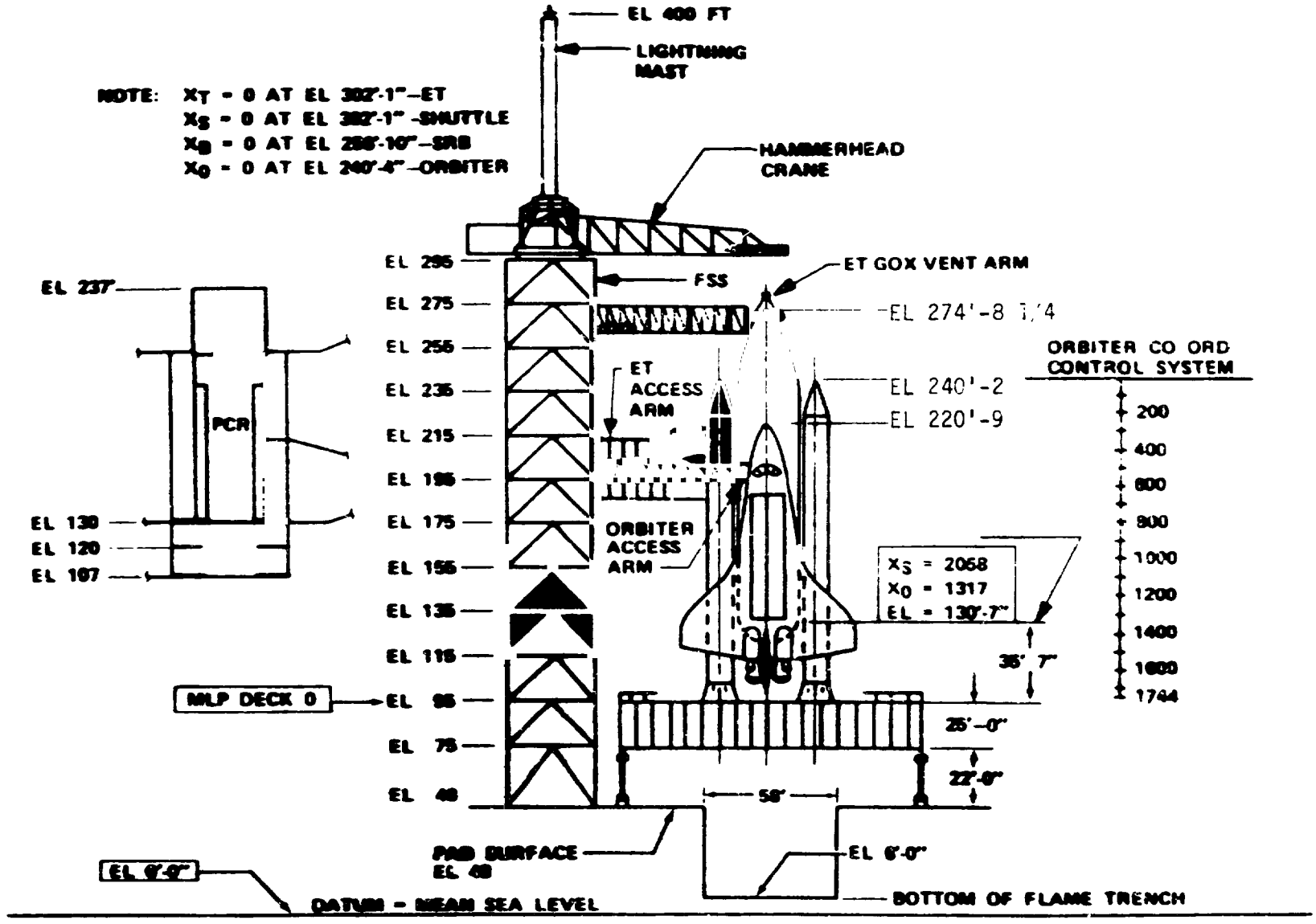

Figure 5. Space Shuttle/Pad Coordinate System

Figure 6. Feedline and Cable Trays

Figure 6. Continued

pressure by vents located throughout the test section. Atmospheric pressure was therefore used as reference pressure for all tests. The processes associated with scanivalve control and pressure measurement were fully automated. A Perkin-Elmer computer was used to drive the scanivalves, stepping all three simultaneously. The computer also records the pressures before stepping to the next set of ports. For each port, 100 pressure samples are taken at 4 milisecond intervals and the average value is calculated and stored.

The pressure transducers were calibrated at least daily, the calibration being rejected of an error of 1% or larger was found at any of the calibration points. Pressure readings were accurate to 0.05 psf. Calibration was checked before each test run and the transducers recalibrated if necessary.

A test run was initiated by measuring and recording pressures at all ports with no wind in the tunnel. After calibration was checked the wind tunnel was started. Once steady conditions were established, pressures at all ports were taken and recorded. The tunnel was then shut off, wind-off pressures were again recorded and calibrations checked.

Cases Studied

The 54 pressure test runs made in the wind tunnel covered the same range of parameter values as the flow visualization runs. The influence of one additional parameter, nozzle size, was studied for the nominal configuration. Tables 5, 6 and 7 list all the cases run and their identifying parameters.

Pressure data is presented in this report as plots of differential pressure vs. location. As previously done for the flow visualization

data, the runs have been organized in groups designed to show the influence of a certain parameter. In this manner, pressure data is presented in groups of runs, each group of runs consisting of eight different plots showing the values of the pressure at different locations of the ET. The groups were organized as follows:

Nominal Configuration

I) Influence of nozzle size, no wind

Runs 11, 12.1 and 13

II) Influence of nozzle size on wind penetration

Runs 7, 9.1, 5 and 8

III) Influence of nozzle pressure on wind penetration

Runs 6.1, 6.2 and 6.3

IV) Wind velocity effects at 338°

Runs 12.1, 3, 1 and 2

V) Nozzle pressure effects, no wind

Runs 12.1, 12.2 and 12.3

VI) Wind velocity effects at 112°

Runs 12.1, 17.1, 17.2, 17.3 and 17.4

VII) Wind velocity effects at 202°

Runs 12.1, 14, 16.1, 15 and 16.2

VIII) Wind velocity effects on wind penetration

Runs 5 and 6.1

IX) Nozzle azimuth angle effects

Runs 1.1, 4 and 5

Variable Nozzle Size Configuration

X) Nozzle pressure effects

Runs 28.1, 28.2 and 28.3

XI) Nozzle azimuth angle effects

Runs 28.1, 29.1 and 30.1

XII) Influence of nozzle pressure on wind penetration for a -15° nozzle azimuth angle

Runs 29.1, 29.2 and 29.3

XIII) Influence of nozzle pressure on wind penetration for a -30° nozzle azimuth angle

Runs 30.1, 30.2 and 30.3

Marshall Space Flight Center Configuration

XIV) Wind velocity effects at 0°, low flowrate

Runs 33.1 and 33.2

XV) Wind velocity effects at 338°, low flowrate

Runs 34.1 and 34.2

XVI) Wind velocity effects at 180°, low flowrate

Runs 35.1 and 35.2

XVII) Wind velocity effects at 90°, low flowrate

Runs 36.1 and 36.2

XVIII) Wind velocity effects at 90°, high flow rate

Runs 37.1 and 37.2

XIX) Wind velocity effects at 180°, high flowrate

Runs 38.1 and 38.2

XX) Wind velocity effects at 338°, high flowrate

Runs 39.1 and 39.2

XXI) Wind velocity effects at 0°, high flowrate

Runs 40.1 and 40.2

XXII) Flowrate effects at 7 KT

Runs 34.1 and 39.1

XXIII) Flowrate effects at 20 KT

Runs 34.2 and 39.2

XXIV) Wind direction effects at 7 KT, low flowrate

Runs 33.1, 36.1, 35.1 and 34.1

XXV) Wind direction effects at 7 KT, high flowrate

Runs 40.1, 37.1, 38.1 and 39.1

XXVI) Wind direction effects at 20 KT, low flowrate

Runs 33.2, 36.2, 35.2 and 34.2

XXVII) Wind direction effects at 20 KT, high flowrate

Runs 40.2, 37.2, 38.2 and 39.2

XXVIII) Flowrate effects, no wind

Runs 32.1 and 32.2

The eight plots included in each group present data for the following locations:

Plot No. 1. Centerline ($\theta = 0$)

Plot No. 2. Axial data for $\theta = 40°$ and $45°$

Plot No. 3. Axial data for $\theta = -40°$ and $-45°$

Plot No. 4. Circumferential data for $X_T = 793$

Plot No. 5. Circumferential data for $X_T = 1273$

Plot No. 6. Circumferential data for $X_T = 1669$

Plot No. 7. Limited Circumferential data for $X_T = 1933$

Plot No. 8. Limited Circumferential data for the ogive at $X_T = 427$ and $X_T = 514$

In addition to all the above mentioned groups, two additional groups of data are also presented:

- Axial pressure data for three circumferential locations close to the feedline, for all runs

- Base pressure data for all Marshall Configuration runs.

HOT FILM MEASUREMENTS

Hot film techniques were used to probe the velocity and temperature fields around the ET. The geometry of the Launch/Pad Shuttle models and the need to make both axial and circumferential surveys made it necessary to probe the flow field from the top of the wind tunnel. Therefore, a suitable probing system had to be developed.

Temperature and velocity measurements were made using a TSI Model 1054B constant temperature amemometer with a model 1040 Temperature Switching Module. A Model 1210-20 hot film probe was used as a sensor.

Only the component of the velocity parallel to the ET surface was measured. Centerline measurements were taken at a distance 0.425 inches from the ET surface approximately. All other measurements were made at a distance of 0.090 inches from the ET surface approximately.

It must be noted that the flow field was highly turbulent in the areas affected by jet impingement, particularly the ET-Orbiter gap. Turbulence levels were, in many cases, above 50% and in general, well above 20%. It is impossible to adequately correct the time-averaged velocity values obtained with the hot film for the effects of this high level of turbulence. No attempt has been made here to provide such a correction and therefore it should be noted that the data here presented has not been corrected for turbulence effects.

Procedure

Routine hot film operating procedures were used throughout the tests. Hot film probes were calibrated before testing began and the calibration checked once it ended. No significant discrepancies were found. Probe location for these measurements was chosen to coincide with pressure tap locations whenever possible so that pressure-velocity correlations could be made.

The probe was positioned manually at the desired location and after a suitable time velocity, turbulence and temperature were measured and recorded using a 4 channel digital voltmeter.

Cases Studied

The process of manually locating the probe was delicate and time consuming, therefore only a limited number of tests were run. For the Nominal Configuration the 338° and 112° cases were studied. For the Marshall Space Flight Center Configuration the 0° wind direction at 20 knots were studied for the high flowrate condition.

HEAT TRANSFER ANALYSIS

It is obvious that the determination of the heat transfer coefficient for such a complex flow field as the one generated by the proposed Norman Engineering ISS is far from trivial. Due to the geometric complexity and the highly interactive flow field created by the jets and the prevailing wind there seems to be no analytical or experimental work readily applicable to the problem.

Bearing this in mind, it is clear that any analysis should be of a highly simplified nature while, at the same time, providing us with reasonable results.

Previous work by Norman Engineering had considered the problem from the point of view of forced convection around circular cylinders. It was felt that the present analysis should try to study the problem from a different perspective and avoid duplicating Norman Engineering's work.

The basic heat transfer mechanism arising from Norman Engineering concept is that of jet impingement. It seems then natural to try and use available jet impingement heat transfer data to the problem at hand and obtain from it an estimate of the heat transfer coefficient.

The utilization of this approach required the following simplifications:

a) The effects of the incoming wind are not considered. This implies that the system is capable of penetrating low velocity winds. In most cases this simplification will lead to conservative values of the heat transfer coefficient.

b) The jets do not interact with each other before impingement. This assumption allows the independent study of each jet and should yield conservative estimates of the heat transfer coefficient.

Flow visualization photographs show that, in the absence of wind, the surface of the ET facing the Orbiter is washed by the jet plumes, the regions affected by each jet being readily distinguishable. In the following, two different procedures will be used to estimate the impingement heat transfer in those regions.

I. The heat transfer rates of a jet impinging normal to a flat plate were studied by Donaldson, et al.(1). A wide range of nozzle exit velocities and impact distances were studied. Their results

are applicable to the present study if we consider the curvature effects of secondary importance and if we are only interested on the mean value of the heat transfer coefficient (Korger and Krizek (2) showed that the integral mean heat transfer coefficient is independent of impact angle).

The experimental results presented in Reference 1 were applied to the case corresponding to the maximum cruise thrust setting of the turbojet engines. Such condition is equivalent to a stagnation pressure setting of 31.2 psia and a nozzle exit temperature of 1340°R.

Under these conditions the heat transfer coefficient for all points located at a distance of 27 feet from the impingement point of the jet exhausting from nozzle No. 1 (i.e., the one for which impingement distance is the shortest) was calculated to be 16.55 $\frac{BTU}{hr°F\ ft^2}$. The heat transfer coefficient for all points located at a distance of 41 feet from the impingement point of the jet exhausting from nozzle No. 6 (i.e., the one for which impingement distance is the largest) was calculated to be 10.9 $\frac{BTU}{hr\ ft^2\ °F}$.

The nature of impingement heat transfer processes is such that all points located at shorter distances from the impingement point will benefit from higher heat transfer rates.

II. Martin (3) used the impingement heat transfer measurements of Gardon and Cobonpue (4), Petzold (5), Brdlick and Savin (6) and Smirnow et al. (7) to obtain the following correlation for the integral mean values of the heat transfer coefficient for single round nozzles:

$$\frac{\overline{N_u}}{P_r^{0.42}} = \frac{D}{r}\ \frac{1-1.1D/r}{1+0.1(H/D-6)D/r}\ F(Re)$$

where: D is the nozzle diameter

r is the radial distance from the impingement point

H is the impingement distance

F(Re) is a function of the Reynolds number.

For the Reynolds number range 120,000<Re<400,000 the value of F(Re) is

$$F(Re) = 0.151\ Re^{0.775}$$

Unfortunately the Reynolds number for our problem is one order of magnitude above the range covered by this formula. We can, however, use this correlation while keeping in mind that it will yield conservative values for the mean heat transfer coefficient. Use of this correlation to evaluate the mean heat transfer coefficient for of 27 ft. radius and with center at the impingement point of jet No. 1 yields:

$$\bar{h} = 10.9\ \frac{BTU}{hr\ ^\circ F\ ft^2}$$

The mean value of the heat transfer coefficient for a circle of 41 ft. radius and centered at the point of impingement of jet No. 6 was determined to be

$$\bar{h} = 7.23\ \frac{BTU}{hr\ ^\circ F\ ft^2}$$

The agreement of the two methods used in these calculations is quite reasonable if we consider that the first one uses far field values for the determination of h, while the second one uses only nozzle exit data and that beforehand we expected the second method to yield conservative values for $\bar{h}$.

Conclusion

The results of the preceeding analysis seem to indicate that the design proposed by Norman Engineering Co. should be capable of

generating values of the heat transfer coefficient for most of the ET facing the Orbiter above 4 BTU/hr ft^2 °F. The presence of wind should, in almost all cases, contribute to higher values of the coefficient of heat transfer. While the existence of small regions of low heat transfer due to stagnant or separated flow is possible, such regions could easily be eliminated by a cyclic variation of jet incidence angle. The implementation of such a system should be strongly considered.

REFERENCES

1. Donaldson, C.duP., Snedeker, R.S., and Margolis, D.P., "A Study of Free Jet Impingement. Part 2. Free Jet Turbulent Structure and Impingement Heat Transfer", J. Fluid Mech., 45, 1971, pp. 477-512.

2. Korger, M. and Krizek, F., Verfahrenstechnik (Mainz)6, 223(1972).

3. Martin, H., "Heat and Mass Transfer between Impinging Gas Jets and Solid Surfaces", Advances in Heat Transfer, 13, Academic Press, New York, 1977, pp. 1-60.

4. Gardon, R. and Cobonpue, J., International Developments in Heat Transfer, p. 454, Am. Soc. Mech. Eng., New York, 1962.

5. Petzold, K., Wiss. Z. Tech. Univ., Dresden 13, 1157(1964).

6. Brdlick, P.M. and Savin, V.K., Inzh.-Fiz. Zh. 8, 146(1965).

7. Smirnov, V.A., Verevochkin, and Brdlick, P.M., Int. J. Heat Mass Transfer 2, 1(1961).

FLOW VISUALIZATION

NOMINAL NOZZLE CONFIGURATION

NO WIND, ZERO AZIMUTH ANGLE

LAB RUNS

RUN	PRESSURE (psia)	NOZZLE SIZE
A	32	Nominal
B	32	Large
C	32	Small
D	27	Nominal
E	27	Large
F	27	Small
G	20	Nominal
H	20	Large
I	20	Small

TABLE 1

FLOW VISUALIZATION

NOMINAL NOZZLE CONFIGURATION

V = Velocity (KNOTS) p = pressure (psia) ϕ = azimuth (°) β = WIND ANGLE (°)

RUN	V	p	ϕ	β
3	20	32	0	338
4	30	32	0	338
5	10	32	0	338
6	20	20	0	338
7	20	27	0	338
8	20	32	-15	338
9	20	32	-30	338
10	30	32	-30	338
11	30	27	-30	338
12	30	20	-30	338
13	20	0	/	338
2	20	32	0	202
14	20	0	/	202
15	30	32	0	202
16	10	32	0	202
1	20	32	0	112
17	20	0	/	112
18	30	32	0	112
19	10	32	0	112

TABLE 2

FLOW VISUALIZATION

VARIABLE NOZZLE SIZE CONFIGURATION

V = Velocity (KNOTS) p = Pressure (psia)

ϕ = Azimuth (°) β = Wind Angle (°)

Nozzle Arrang.: Lower 3, Small; Middle 2, Nom.; Upper, Large

RUN	V	p	β	ϕ
48	0	32	/	/
49	0	27	/	/
50	0	20	/	/
51	20	32	338	-30
52	20	27	338	-30
52	20	20	338	-30

TABLE 3

FLOW VISUALIZATION

MARSHALL SPACE FLIGHT CENTER CONFIGURATION

V = Velocity (KNOTS)

β = Wind Angle (°)

Flowrate: H (High), L (Low)

RUN	V	Flowrate	β
44	0	H	/
45	7	H	338
46	20	H	338
47	0	L	/

TABLE 4

PRESSURE MEASUREMENTS

NOMINAL NOZZLE CONFIGURATION

V = Velocity (KNOTS) p = Pressure (psia)

ϕ = Azimuth (°) β = Wind Angle (°)

Nozzle Size: L (Large), N (Nominal), S (Small)

RUN	V	p	β	ϕ	Nozzle Size
1	20	32	338	0	N
2	30	32	338	0	N
3	10	32	338	0	N
4	20	32	338	-15	N
5	20	32	338	-30	N
6.1	30	32	338	-30	N
6.2	30	27	338	-30	N
6.3	30	20	338	-30	N
7	20	0	338	/	/
8	20	32	338	-30	L
9.1	20	32	338	-30	S
9.2	20	27	338	-30	S

TABLE 5

PRESSURE MEASUREMENTS

NOMINAL NOZZLE CONFIGURATION

V = Velocity (KNOTS) P = Pressure (psia)

ϕ = Azimuth (^{o}) β = Wind Angle (^{o})

Nozzle Size: L (Large), N (Nominal), S (Small)

RUN	V	p	β	ϕ	Nozzle Size
10	30	32	338	-30	S
11	0	32	/	0	S
12.1	0	32	/	0	N
12.2	0	27	/	0	N
12.3	0	20	/	0	N
13	0	32	/	0	L
14	20	0	202	/	/
15	20	32	202	0	N
16.1	30	32	202	0	N
16.2	10	32	202	0	N
17.1	20	0	112	/	/
17.2	20	32	112	0	N
17.3	30	32	112	0	N
17.4	10	32	112	0	N

TABLE 5 (CONTINUED)

PRESSURE MEASUREMENTS

VARIABLE NOZZLE SIZE CONFIGURATION

V = Velocity (KNOTS) p = Pressure (psia)

ϕ = Azimuth (°) β = Wind Angle (°)

Nozzle Arrang.: Lower 3, Small; Middle 2, Nom.; Upper, Large

RUN	V	p	β	ϕ
27(1,2)	20	32	338	0
28.1	20	32	338	0
28.2	20	27	338	0
28.3	20	20	338	0
29.1	20	32	338	-15
29.2	20	27	338	-15
29.3	20	20	338	-15
30.1	20	32	338	-30
30.2	20	27	338	-30
30.3	20	20	338	-30

TABLE 6

PRESSURE MEASUREMENTS

MARSHALL SPACE FLIGHT CENTER CONFIGURATION

V = Velocity (KNOTS)

β = Wind Angle (^{o})

Flowrate: H (High), L (Low)

RUN	V	FLOWRATE	β
32.1	0	H	/
32.2	0	L	/
33.1	7	L	0
33.2	20	L	0
34.1	7	L	338
34.2	20	L	338
35.1	7	L	180
35.2	20	L	180
36.1	7	L	90
36.2	20	L	90
37.1	7	H	90
37.2	20	H	90
38.1	7	H	180
38.2	20	H	180
39.1	7	H	338
39.2	20	H	338
40.1	7	H	360
40.2	20	H	360

TABLE 7